Chapter 4

To isolate fibers from natural sources and prepare fiber-reinforced composite films of starch/protein blends

4.1. Introduction

The growing global concern about plastic waste has driven interest in renewable resources to develop sustainable solutions for protecting the ecosystem. Biodegradable polymers present a promising alternative to synthetic plastics, with starch being one of the most well-known renewable resources. However, starch-based films suffer from drawbacks such as brittleness, moisture sensitivity, and poor processability, limiting their use in packaging applications. To address these issues, researchers have explored blending starch with other substances to enhance mechanical strength and flexibility (Azevedo et al., 2022). Natural fibers have emerged as viable reinforcements for polymer composites, offering an eco-friendly substitute for synthetic fibers (Bekraoui et al., 2022). Reinforcing cellulosic fibers with biopolymers led to improvement in mechanical characteristics, making them suitable for usage in food, biomedical, including pharmaceutical areas (Ren et al., 2023). However, poor adhesion between fibers and polymer matrices remains a challenge (Fazeli and Simao, 2019). Fiber modifications, such as enzymatic treatments, have been explored to enhance compatibility and processing efficiency. BPF (banana-pseudostem fiber), a lignocellulosic fiber extracted from banana plant pseudo-stems, exhibits high strength, strong moisture absorption, and excellent biodegradability, making it a potential candidate for composite films (Saxena and Chawla, 2021). Similarly, bamboo-shoot fiber (BSF), with its high cellulose content (40-50%), has gained attention as a sustainable alternative for packaging materials (El Foujji et al., 2021). Incorporating natural fibers into packaging films reduces environmental impact and enhances mechanical strength and thermal stability compared to traditional materials like polylactic acid (PLA) (Fei et al., 2023).

The ultrasound technique is a green, rapid, and energy-efficient processing method that enhances film solubility and structure by creating compact net-like formations (Kang et al., 2023). This technique results in smoother, denser films with improved mechanical and barrier properties (Liang et al., 2021). Additionally, enzymatic treatments using cellulase, composed of β-glucosidase (GB), cellobiohydrolase (CBH), and endoglucanase

(EG), help degrade cellulose, increasing fiber fluidity and improving bio-composite performance (Ghosh et al., 2024; Li et al., 2022). Enzymatic treatments soften and swell raw materials, further enhancing fiber compatibility (Bian et al., 2020). To optimize reinforcement, improving fiber and matrix properties is essential to ensure strong adhesion and meet packaging requirements. Current research focuses on developing innovative materials with tailored properties to meet the evolving needs of the packaging industry (Norrrahim et al., 2024). The combined application of ultrasound and enzymatic treatments presents a promising approach for reinforcing natural fibers in biopolymers, offering a sustainable, efficient, and adaptable method (Li et al., 2024). Thus, the objective of this chapter is to explore ultrasound and enzyme treatments, individually and in combination, for enhancing the compatibility and contact between the natural fibers (banana pseudostem and bamboo-shoot), starch, and casein. This approach aims to develop bio-composite films with improved mechanical properties for diverse applications in food packaging and environmental engineering. The ultimate goal is to identify the best treatment combinations for optimizing fiber-film formulations, thereby enhancing the overall performance and functionality of biodegradable films.

4.2. Materials and methods

4.2.1. Materials

The banana pseudostem was collected from a nearby banana plantation plot (Tezpur University, Napaam, Assam, India). A local bamboo plantation plot (Tezpur University, Napaam, Assam, India) provided the bamboo shoots for the experiment. Casein (CN, purity > 90%) was purchased from Zenith India, Guwahati, Assam, India.

4.2.2. Chemical and reagents

Analytical-grade reagents and chemicals, purchased from Zenith India, Guwahati, Assam, India, were utilized throughout the study.

4.2.3. Extraction of banana pseudostem fiber (BPF)

The extraction of BPF was performed according to the method of Fazeli et al. (2018) with some modifications. Dewaxed BPF were cleaned with DW and then allowed to dry dried at ambient temperature after being dewaxed for 72 h in a 3:1 toluene/ethanol

mixture. Once the fibers got dried, they were trimmed into 6 mm short fibers. Lignin including hemicelluloses were extracted by treating the material with a 5% NaOH solution at 60°C for 8 h. Following the washing process, 3M HCl was utilized to break down cell walls and isolate micro-fibrils. Further using DI water, the fibers were washed well to remove the acidic solution. Further, the fibers are then ground into pulp and subjected to another alkali treatment to eliminate any remaining non-cellulosic components, followed by acid hydrolysis using a 5 M acid solution. The delignification was further performed by the bleaching procedure. After delignification, fibers were bleached with a 5:1 mixture of sodium hypochlorite ($NaClO_2$) and glacial acetic acid for 4 h at 50℃. After bleaching, the fibers were thoroughly washed with deionized water until a neutral pH of 7 was achieved.

4.2.4. Extraction of bamboo-shoot fiber (BSF)

The steps for extracting BSF were systematically carried out according to the protocol of Hu et al. (2019). Initially, the shoots underwent a dewaxing process by immersing them in a toluene and ethanol mixture (3:1, v/v) for 72 h duration at a temperature of 45ºC. This was then treated with 5% NaOH at 60ºC for 8 h to remove lignin and hemicellulose from the material. Microfibrils were then isolated using 3 M HCl, followed by grinding into pulp. The pulp was treated with alkali and acid hydrolysis using 5 M HCl. The next step involved bleaching, where a 5:1 mix ratio of sodium hypochlorite and glacial acetic acid was applied for 4 h at 5℃. Finally, homogenization was performed at 2200×g rpm for 4 h for achievement of desired material characteristics. This comprehensive procedure ensured the preparation of BSF with the desired characteristics for further applications.

4.2.5. Ultrasound treatment (US) of natural fibers

Homogenized BPFs and BSFs were treated with ultrasound following the procedure of Twebaze et al. (2022) with some alterations. The above-homogenized fiber (5%) dry weight basis was treated with 60% amplitude frequency for 15 min. Treated fibers were then centrifuged and dried. Further, it was stored in air-tight containers for analysis.

4.2.6. Enzymatic treatment (ET) of natural fibers

According to the procedure of Li et al. (2022), BPFs and BSFs were enzymatically treated. Cellulase enzymes used for the experiment were first diluted to 10 mL. BPFs and BSFs were homogenized using a homogenizer and stored for refrigeration. The amount of cellulase enzyme used for treatment was 1 mL diluted to 10 mL. Homogenized fibers (5%) were dispersed in 1 mL diluted enzyme solution. After this, the medium was immediately incubated for 30 min at 45℃. To inactivate the enzymes, the dispersed fibers were submerged in a boiling water bath for 5 min. They were then chilled in an ice bath, centrifuged for 15 min at 9000 rpm, and thoroughly cleaned with DW. For further examination and integration into the composite films, the resultant fibers were kept in airtight containers.

4.2.7. Preparation of (PS)-fiber (banana-pseudostem/bamboo-shoot) reinforced composite films

Potato starch and BPF/BSF composite film were produced by solvent casting technique as per the method of Balakrishnan et al. (2017). Potato starch (5%) composition was put inside a 250 mL conical flask which was kept for stirring at a constant 300 rpm for 15 min at 90 °C using a magnetic stirrer to achieve complete gelatinization of the starch. The calculated weight percentage (5 % on a dry weight basis) of BPF and BSF fibers (treated and untreated) were dispersed in DW and stirred separately at a magnetic stirrer at 60℃ for half an hour. Glycerol at the concentration of 40 mL 100 g^{-1} (of dry starch to the solution) was added to avoid film brittleness. The suspension of BPF and BSF fiber (treated and untreated) was poured into the starch-glycerol water mixture and stirred for 30 min at 90℃ using a mechanical stirrer set to 700 rpm. It was then poured onto leveled glass petri plates after the solution became viscous, and dried at 45℃for 12 h. The films were then removed from the petri plates and kept inside the incubator for conditioning at around 65% RH at 25℃ temperatures. The films conditioned were put inside a desiccator (56% RH) for one week at 30℃. The PS films reinforced with BPF and BSF fibers were then analyzed for various film properties.

4.2.8. Characteristics of extracted fiber (banana-pseudostem and bamboo-shoot)

4.2.8.1. Solubility

Solubility was measured corresponding to the procedure of Patel and Joshi (2020) following a few modifications. The fibers (banana and BSF, native and treated) were measured and put in a 50 mL beaker containing 10 mL DW. The mixture was kept in a shaking incubator with a speed of 250 rpm at 30℃ for 4 h. Centrifugation at 6000 rpm was done thereby for 10 min. After 4 h of drying at 105℃, the pellet was weighed. The weight of insolubilized dry matter was subtracted from the initial dry matter weight to determine the weight of solubilized dry matter, which was then expressed as a percentage of the total weight.

4.2.8.2. Water holding capacity (WHC)

Native and treated (BPF and BSF) water holding capacity was evaluated by the method of Afrin et al. (2022) with alterations. Fiber (1 g) was dissolved in 10mL of DW and centrifuged for 30 min with agitation for a few seconds. The materials were kept for centrifugation for 25 min at 3000g after 30 min.

Finally, water holding capacity of the BPFs was determined using the Equation below:

$$\text{Water holding capacity \%} = \frac{\text{Weight of the tube after release of supernatant}}{\text{Weight of the tube with sample before addition of water}} \times 100 \quad (4.1.)$$

4.2.8.3. Oil holding capacity (OHC)

Native and treated (BPF and BSF) oil-holding capacity was evaluated by Singha et al. (2023) including some alterations. In pre-weighed centrifuge tubes, 0.5 g of native and modified banana and BSFs were mixed with 6 mL of sunflower oil. For full dispersion of the sample in oil, the tubes were agitated for one min. The samples were centrifuged at 3000g for 25 min following a 30 min holding period. Before reweighing the tubes, the supernatant was pipetted and left upside down for the oil to drain completely up to 25 min. Oil absorption was determined based on oil absorption per gram of fiber as per the following Equation **(4.2)**.

$$\text{Oil holding capacity \%} = \frac{\text{Weight of the tube after released of supernatant}}{\text{Weight of the tube with sample addition of oil}} \text{x}100 \quad (4.2)$$

4.2.8.4.Scanning electron microscopy (SEM)

The microstructure of the banana and BSF (treated and native) was analyzed using a scanning electron microscope (SEM) (JEOL, Japan Model: JSM) with varying magnification and at an accelerating voltage of 15 kV up to 1000X by Pathaw et al. (2023).

4.2.8.5. X-ray diffraction (X-RD)

For examination of the potential differences in crystalline organization, crystallinity including relative dimensions of the native and treated BPF, a powdered X-ray diffractometer (D8 FOCUS, Bruker Axs, Germany) was performed. With a sampling interval of 0.02º and a scanning velocity of 0.25º/min, the 2θ scan was carried out from 5º to 35º as described by Choi et al. (2020).

4.2.8.6. Fourier transform infrared spectroscopy (FT-IR)

Evaluation of the functional groups present in the fiber (native and treated) was carried out by an infrared Fourier-transform spectrometer (FTIR) (IMPACT 410, Nicolet, USA) in the IR region (4000-500 cm^{-1}) with a resolution of 4 cm^{-1} as demonstrated by Chutia and Mahanta (2021). By measuring the height of the spectra's absorbance bands relative to the baseline, intensity analysis was made.

4.2.8.7. Thermal properties

Thermogravimetric measurements of the native and modified Banana and BSF were performed using TGA (thermogravimetric analyzer) equipment (Netzsch TG 209F1D-0294-L) employing the method of Liu et al. (2021). For each experiment, 10-12 mg of samples were added to a standard alumina pan. The pan was then heated at a rate of 10°C per minute from 300°C to 600°C while a nitrogen flow of 50 mL/min was in place. The samples were examined three times, with an empty pan acting as a reference.

4.2.9. Preparation of casein and fiber (banana-pseudostem/bamboo-shoot) reinforced composite films

The solvent-casting technique procedure outlined by Cho et al. (2014) with some alterations applied to prepare composite films using casein and native and modified BPF and BSF. Casein was initially stirred in a 0.2% weight aqueous sodium hydroxide solvent at 80℃ for 3 h in a round bottom flask. Simultaneously, homogenized fibers (BPF/BSF) - (5%) were dispersed in D.W. and stirred separately in a magnetic stirrer for 30 min at 40℃. The casein mixture was mixed with the suspension of BPF and BSF (treated and untreated), and the combination was agitated for 30 min at 90℃ at 700 rpm using a magnetic stirrer. Glycerol at a rate of 40 mL/100g was added to the solution to overcome brittleness. Neat composite films were then prepared by casting them onto leveled glass petri plates once the solution became viscous, and the plates were kept at 45℃ for 12 h until complete drying. The solution was then left to dry at room temperature (22 ± 2°C) for 48 h. After being removed from the petri plates, the films were stored at 25°C and around 65% relative humidity (RH) in an incubator after they had dried. After conditioning, the films were placed inside a desiccator (56% RH) for one week at 30°C.

4.2.10. Characteristics of developed film

4.2.10.1.Film thickness

Film thickness has been measured by following the method described in Section 3.2.12.1.

4.2.10.2.Film solubility (%)

Film solubility (%) was measured as the protocol described in Section 3.2.12.1.

4.2.10.3. Optical properties

The optical property of the developed film has been evaluated by the method detailed in Section 3.2.12.4.

4.2.10.4. Mechanical properties

The tensile strength (TS) and elongation at break (EAB) % of the developed film

has been determined by the method detailed in Section 3.2.12.5.

4.2.10.5. Sealing properties

The sealing strength determination of the developed film has been determined following the method described in the section 3.2.12.6.

4.2.10.6. Water vapor permeability (WVP)

The WVP of the film developed has been evaluated as per the process described in Section 3.2.12.2.

4.2.11. Statistical Analysis

SPSS statistical software (version 26, SAS Institute Inc., Cary, NC, USA) was employed to obtain the experimental data indicated as mean ± standard deviation. One-way (ANOVA) variance and Duncan's multiple range test (DMRT) using a probability ($p<0.05$) were taken into consideration for determining statistical differences.

4.3. Results and Discussion

4.3.1. Properties of native and modified banana-pseudostem and bamboo-shoot fibers

4.3.1.1. Solubility

The potential of natural fibers to retain water is crucial for its food packaging applications. **Tables 4.1 and 4.2** presented the solubility (%) of native and treated BPFs along with BSFs. The results presented depicted significant variations ($p<0.05$) among the samples. The native fibers showed the highest solubility (17.6% and 26.04compared with other samples attributed to the hydrophilicity of the fibers (Li et al., 2022). The solubility of the natural fiber reduced significantly between the treatments for ultrasound and enzyme along with their combination which may be due to the disruption in the hydrophilic groups and BPF crystalline structure (Hu et al., 2019). In the case of ultrasound treatment of BPFs, the solubility decreased significantly from 17.6% to 14.56%, while for enzyme treatment, the solubility of the BPF reduced drastically from 17.6% to 15.52%. The mutual effect of ultrasound and enzyme modification showed a substantial reduction of solubility which

could be attributed to the ultrasonication. The solubility of BPFs was further reduced as the ultrasound power and enzyme treatment combined causing a decrease in the ability to hold water (Ullah et al., 2018) which is a desirable characteristic for packaging. In the case of ultrasound treatment of BSF, the solubility decreased significantly to 18.58%, while for the enzyme modification the solubility of the BSF reduced to 16.52%, respectively. When ultrasound and enzyme therapy were applied together, the solubility of ETUS (18.65%) and USET (15.24%) was significantly reduced overall. The hydrophilic character of the fiber is significantly reduced throughout the extraction process by alkali treatment, resulting in less moisture absorption. According to Liu et al. (2021), the number of hydrophilic components like cellulose and hemicellulose, which were reduced in BSF following cellulase modification, determined the hydration properties of fibers **(Table 4.2)**. Additionally, US can cause the fibers to aggregate and compact, reducing the overall surface area available for interaction with water. This reduction in accessible surface area can lead to a decrease in the solubility of the fibers (Martinez-Solano et al., 2021). Ultrasound treatment significantly improved soluble DF in okara fibers which reduced the accessibility of the fiber's internal structure to water, resulting in a lower solubility (Fan et al., 2020). First, greater surface tension strength produced a more porous fiber capillary structure, which in turn led to better solubility of natural fibers used. Because of the BSF's increased porosity, the surface tension improved, which enhanced the capillary force. In conclusion, after cellulase modification, BPF along with BSF's hydration capabilities were improved due to a more porous surface structure, an increase in reactive groups, and a larger exposure to water-binding sites induced by a decrease in crystallinity (FTIR **Fig. 4.1 and 4.2**) (Aguado et al., 2019). Thus, upon modification fiber solubility was reduced, which shows it is less susceptible to dissolution or disintegration when exposed to moisture or water. This enhanced water resistance is important for maintaining the structural integrity including barrier properties of fiber-based food packaging materials, ensuring their ability to effectively protect packaged food.

Table 4.1 Physico-chemical properties of BPF

Parameters	Fiber (Native and modified)				
	N	**US**	**ET**	**USET**	**ETUS**
Solubility (%)	17.6 ± 1.98^{a}	14.56 ± 0.79^{b}	15.52 ± 0.51^{b}	14.04 ± 0.28^{bc}	13.65 ± 0.13^{c}
Water holding capacity (WHC) (%)	142.63 ± 2.23^{a}	126.91 ± 0.89^{c}	133.72 ± 1.02^{bc}	122.69 ± 0.52^{c}	136.66 ± 0.98^{b}
Oil Holding Capacity (OHC) (%)	145.61 ± 1.52^{a}	122.53 ± 1.01^{c}	132.69 ± 0.93^{b}	120.67 ± 0.57^{c}	117.14 ± 0.76^{d}

Means depicted by different superscript small letters within the column are significantly different ($p<0.05$). (BPF- Banana pseudostem-fiber, N- Native fiber, US- ultrasound treated fiber, ET- Enzymatic treated fiber, USET- ultrasound combined with enzyme treatment, ETUS- Enzyme treatment combined with ultrasound treatment)

Table 4.2 Physico-chemical properties of BSF

Parameters	BSF (Native and modified)				
	Native	**US**	**ET**	**USET**	**ETUS**
Solubility (%)	26.04±1.26^{a}	18.58±0.59^{b}	16.52±0.34c	15.24±0.38^{bc}	18.65± 0.23^{b}
Water holding capacity (WHC) (%)	163.36±2.23^{a}	145.91±1.89^{c}	152.72±1.32^{bc}	149.69±1.11^{c}	156.66±1.98^{b}
Oil Holding Capacity (OHC) (%)	142.61±1.52^{a}	128.53±1.21^{c}	138.69±1.63^{b}	122.67±1.57^{d}	136.14±1.12^{b}

Means depicted by different superscript small letters within the column are significantly different ($p<0.05$). (BSF-Bamboo-shoot fiber, N- Native fiber, US- ultrasound treated fiber, ET- Enzymatic treated fiber, USET- ultrasound combined with enzyme treatment, ETUS- Enzyme treated with ultrasound treatment)

4.3.1.2. Effect on WHC (Water holding capacity) and OHC (Oil holding capacity)

Functional properties (WHC and OHC) of treated and untreated fibers used (banana and bamboo shoots) are presented in **Tables 4.1 and 4.2**. Data depicted significant differences ($p<0.05$) between the samples. A low oil-holding capacity and water-holding capacity of the fiber is beneficial for film development, and retaining oil during food processing. In the case of BPF, the ultrasonication resulted in a decrease in WHC (126.91%) and OHC (122.53%) which may be attributed to the destruction of the BPF channels and its porous structure reducing the ability to trap water in the BPF matrix (Fan et al., 2020). The combination of cellulase enzyme and ultrasonication showed lower WHC and OHC for US+ET (122.69%; 120.67%) and ET+US (136.66%; 117.14%) respectively. Enhancement in pore size and volume of the fibrous matrix due to ultrasound treatment may have led to a higher binding capacity of oil and water (Fazeli et al., 2023). Due to the cellulase enzyme, there is a possibility that the enzymes adsorbed onto the lignin hindered the accessibility and thus prevented the binding of oil/water to cellulosic fibers (Bian et al., 2020). The combined effect of ultrasound and cellulase enzyme can be observed indicating ultrasound that lowered the activity of cellulase enzyme. This is in agreement with the results proposed by Oliveira et al. (2017) and Olguin-Maciel et al. (2022). When BSF (BSFs are exposed to water or oil, the cellulosic fibers tend to swell, leading to the development of shear stresses at the interface, which promotes the ultimate debonding of the fibers, consequently causing a reduction in strength (Bourmad et al., 2020). Native BSF had OHC and WHC of 142.61% and 163.36%. Upon modification with ultrasound and cellulase treatment, WHC and OHC were reduced and became low upon dual modification. The modification (US) induces structural alterations in natural fibers, including disruption of the cell wall and lumen structure. These alterations can decrease the internal surface area and fibers pore volume, which are crucial for their oil and water retention capabilities. Swelling and compaction of natural fibers, particularly inside the amorphous areas of the cellulose structure, are common outcomes of ultrasound treatment (Martinez-Solano et al., 2021). These changes contribute to a reduction in the overall porosity and void spaces within the fibers, consequently yielding stable dispersions while diminishing their water and oil retention capacities (Szymańska-Chargot et al., 2022). Cellulase treatment reduced OHC (138.69%) along with minimum WHC (152.72%). Additionally, upon dual treatment, ETUS reduced low OHC comparatively (136.14%) and WHC (156.66%). The removal of non-cellulosic components facilitated by the cellulase,

as elucidated in FTIR results **(Fig. 4.2 and 4.3)**, can significantly alter the overall chemical composition and structure of fibers. This alteration affects their hydrophilic and hydrophobic properties, subsequently influencing their oil and water retention capacities. Studies have indicated that fibers with low lignin content display reduced OHC when treated with cellulase (Liu et al., 2021). In addition, following cellulase modification, the hydration characteristics (water holding capacity) of the dietary fiber from rice bran were improved because of a more porous surface structure, more reactive groups, and increased exposure of water-binding sites as a result of decreased crystallinity (Tanasa et al., 2019). Cellulase treatment has been successful in improving the WHC (water-holding capacity) and OHC (oil-holding capacity) of the dietary fiber from rice bran (Liu et al., 2021), while also showing decreased values according to findings by Wen et al. (2017) for rice bran dietary fiber. The physical treatment of BSF (ultrasound and cellulase modification) particularly its combination, has enhanced the critical barrier, dimensional, and stability properties required for effective food protection and preservation.

4.3.1.3. Fourier transform infrared spectroscopy (FT-IR)

FTIR is employed for the determination of the effect of the modification on the fiber's surface structure. BPF components comprise esters, alkenes, aromatic, and ketenes including alcohol with various O_2 consisting functional groups (Yusuf et al., 2019). **Fig. 4.2 and 4.3** depict the FTIR spectra of BPFs and BSFs with almost similar spectral regions due to similar fiber characteristics. The main difference typically lies in the relative intensities of these peaks, reflecting slight variations in the proportions of these components between the fibers, but the overall spectral pattern remains similar due to their shared basic chemical composition. Six regions can be taken as major characteristic bands observed among the samples that are 3650-3000 cm^{-1},3337 cm^{-1}, 1797-1507 cm^{-1}, 1282-856 cm^{-1}, 855-401 cm^{-1}, and 666 cm^{-1}. Additionally, these absorption spectra suggest the creation of hydrogen bonds along with uniform dispersion of BSF due to ultrasound and enzyme treatment and with dual treatment (Yasmeen et al., 2016). The larger absorption bands were noticed in the region of 3650-3000 cm^{-1} and 3337 cm^{-1} that showed OH bend and -OH stretching describing hydrophilicity of fiber with specific intramolecular H-bonds of cellulose (waxes and lignins) (Razab et al., 2022). The intensity of the band increased with treatment showing interactions of hydrogen with cellulose. The absorption peak of the C=O stretching was from 1797-1507 cm^{-1} for cellulase enzyme treatment depicting

vibration of acetyl & uronic ester groups of hemicelluloses/ ester linkages of the carboxylic group of lignin that showed carboxyl group content of BPFs had increased. The absence of the peak in ultrasonic treatment may be due to the absence of carboxylic groups. The peaks from 1282-856 cm^{-1} presented C=O stretching presenting the typical structure of celluloses. The presence of aromatic groups of the lignin in BPFs was observed at 855-401 cm^{-1} along with ortho, meta, and para compounds at 666 cm^{-1} for cellulase enzyme treatment. Similar absorbing features and groups were observed for the samples with additional peaks in cellulase enzyme treatment that showed that enzyme treatment affected the chemical structure of BPFs (Li et al., 2022). Furthermore, peaks of treated BSF were more prominent comparatively, which results from treatment effects effectively indicating an augmentation in cellulose content. In BSF, characteristic absorption peaks of lignin, such as the H-O-H in the cellulose acetyl group at 1645 cm^{-1}, ether bond at 906 cm^{-1}, and the symmetric tensile vibration area of aromatic ring C–C at 1604 cm^{-1}, have been observed. The absorption peaks at 1624 cm^{-1} and 1305-1458 cm^{-1}, linked to the C=O group and C–O stretching vibration, respectively, were observed in BSF indicating the elimination of lignin and hemicellulose after treatment (Alattar et al., 2021). Thus, from the FTIR curve, it can be reported that modification of enzyme and ultrasonication treatment of fiber removed lignin and hemicellulose component and led to enhancement of hydrophilic groups like COO−, OH, and C=O that promoted better dispersion property and thus can improve mechanical characteristics of developed films (Liu et al., 2021). The spectral analysis of all the BSF displayed a consistent pattern, suggesting that significant alterations in the functional groups of BSFs did not occur because of the physical modification. These results indicated that ultrasound and its combination with cellulase treatment had better interfacial adhesion comparatively promoting effective dispersion of fibers as reinforcement, formation of hydrogen bonds, and removal of non-cellulosic components, which increased the hydrophobic characteristics. Similar spectra were noticed in the cases of Liu et al. (2021), Yusuf et al. (2019), and Chin et al. (2020) for bamboo fiber composites.

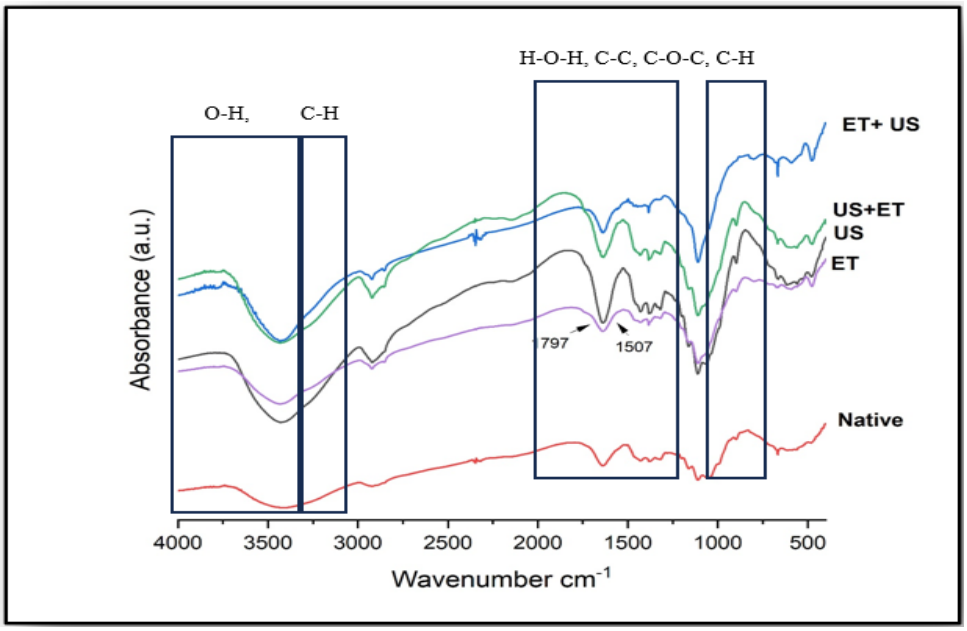

Fig. 4.1 Fourier transform infra-red spectroscopy **(**FTIR) curves of native and modified Banana pseudostem fibers (BPFs)

(N: Native fiber, US: ultrasound treated fiber, ET: Enzymatic treated fiber, USET: ultrasound combined with enzyme treatment, ETUS: Enzyme treated with ultrasound treatment)

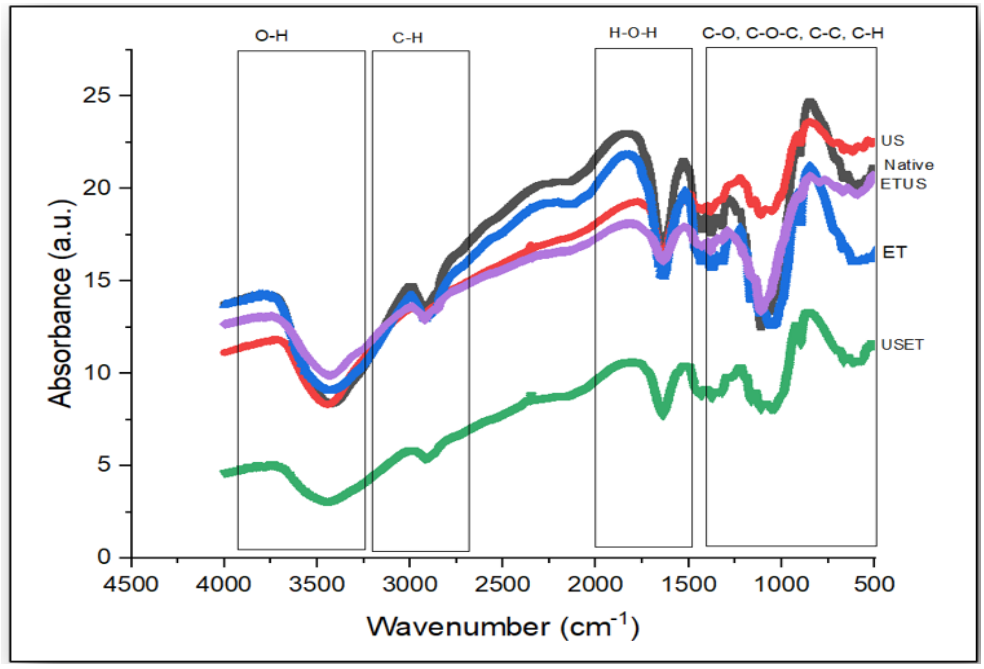

Fig. 4.2 Fourier transform infra-red spectroscopy **(**FTIR) curves of native and modified Bamboo-shoot fibers (BSFs)

(N- Native fiber, US: ultrasound treated fiber, ET: Enzymatic treated fiber, USET: ultrasound combined with enzyme treatment, ETUS: Enzyme treated with ultrasound treatment)

4.3.1.4. Scanning electron microscopy (SEM)

The surface morphology of banana and BSFs modified by ultrasound and enzymatic treatment using scanning electron microscopy are depicted in **Fig. 4.3 and 4.4 (A, B, C, D, and E)** at ×10 and ×100 magnifications. Long filaments with loose structures and cracks were observed in the case of BPFs (Priyadarshana et al., 2022). The BPFs revealed were in the form of polymerized fibrous bundles that were discrete when the fibers were treated with varying degrees of breakage (Li et al., 2022). Modification of BPFs provided a rough structure along with a distinct separation of fibrils compared to untreated ones. The aim of the alteration is to expose the surface region owith a reduction in the hydrophilic groups like lignin. The appearance of irregular and breakage of fibers with increased surface roughness due to treatment of ultrasonication and cellulase enzyme was noted. The rough surface in modified fiber is observed because of the removal of hemicellulose and lignin (Liang et al., 2021). The appearance of irregular and layered strips due to cellulase enzyme could be due to enzymatic disintegration that improved the fibrillation of cellulose (Li et al., 2022; Bian et al. 2020). SEM images of BPFs noticed in this study were similar to those observed in the earlier study (Fan et al., 2020). Ultrasonication-treated BPFs showed cracks on the surface of filamentous fibers loosening the tight structure and ultimately providing space for penetration (Ouyang et al., 2023). The combined treatment of ultrasound and enzyme treatment of the BPF has created dispersion throughout the matrix, causing enormous filler aggregates that resulted in variations in the microscopic morphology (Liang et al., 2021). While for BSF, the fibers exhibited a shape that was almost circular or elliptical, similar to other lignocellulosic fibers like kenaf fibers (Chin et al., 2020). The BSF in **Fig. 4.4** at various magnifications (×10 to ×100), native and modified BSF, exhibited extensive wrapping, resulting in an uneven and rough surface characterized by abundant non-cellulose components like lignin and hemicellulose. Treating fibers with an alkaline solution during modification creates a more exposed or irregularly textured surface. After modification, the majority of the amorphous materials situated between and on the BSF fibers were eliminated, revealing a fiber surface adorned with numerous grooves, thereby imparting certain moisture absorption and release properties (Yang et al., 2022). Results were similar for bamboo-fiber reinforced composites as in Ramesh et al. (2021). The changes thus observed on the surfaces of the BSF can be due to the molecular reorganization of the constituent molecules within the bamboo fibers, as indicated by the FTIR analysis (Owolabi et al., 2018). When

sisal fibers undergo ultrasonic treatment, amorphous elements are eliminated and cellulose is separated or disintegrated, which effectively increases the sisal fibers' surface roughness (Krishnaiah et al., 2017). The mechanical and thermal properties of fiber-reinforced polymer composites can be improved by increasing the adhesion or mechanical interlocking amongst the fiber surface and polymer matrices, which is dependent on an increase in surface roughness (Solis Rosales et al., 2022). Similar findings with other natural fibers have also been reported by other researchers, who saw that enzyme and ultrasonic treatments removed pectin and other components from the fiber surface (Yadav et al., 2022). In addition, they noted irregularities in the fiber surface structure, which further promoted adhesion amongst the fiber and polymer matrices in polymer composites (Lee et al., 2021).

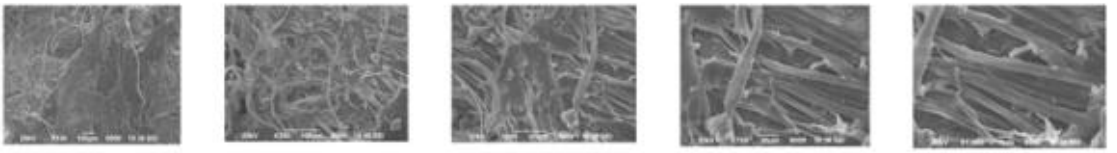

A. Native Fiber

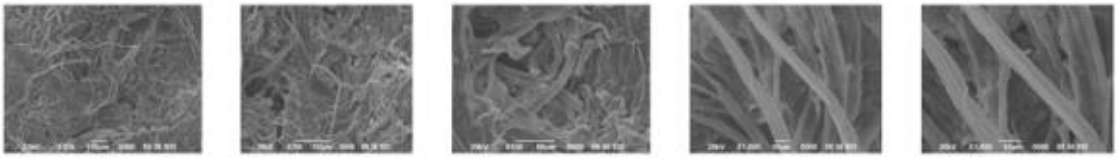

B. US (Ultrasound treated fiber)

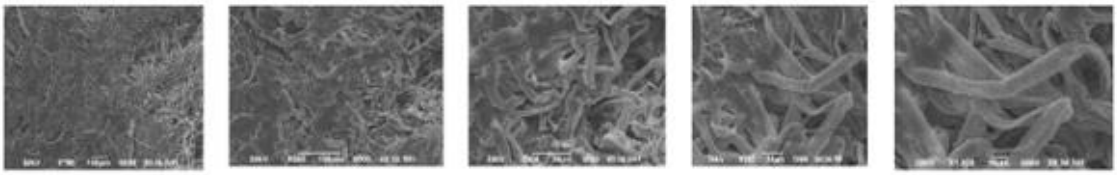

C. ET (Enzyme treated fiber)

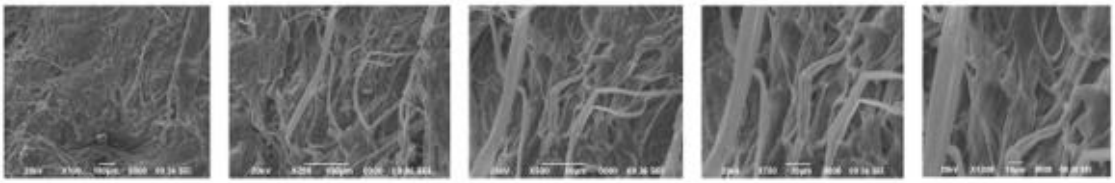

D. USET (Ultrasound treated fiber + enzyme treated fiber)

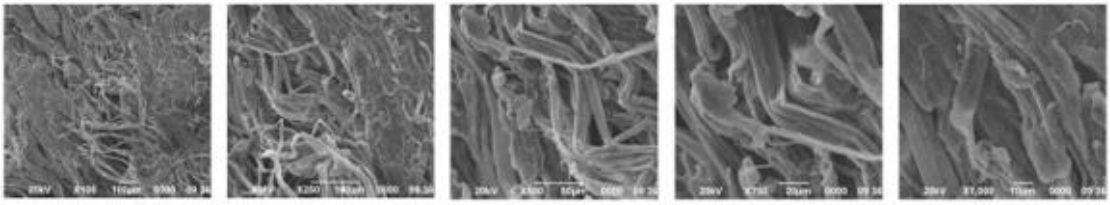

E. ETUS (Enzyme-treated fiber + ultrasound-treated fiber)

Fig. 4.3 (A,B, C,D, and E) Scanning electron microscopy (SEM) images of Banana pseudostem fibers (BPFs) obtained at different magnifications

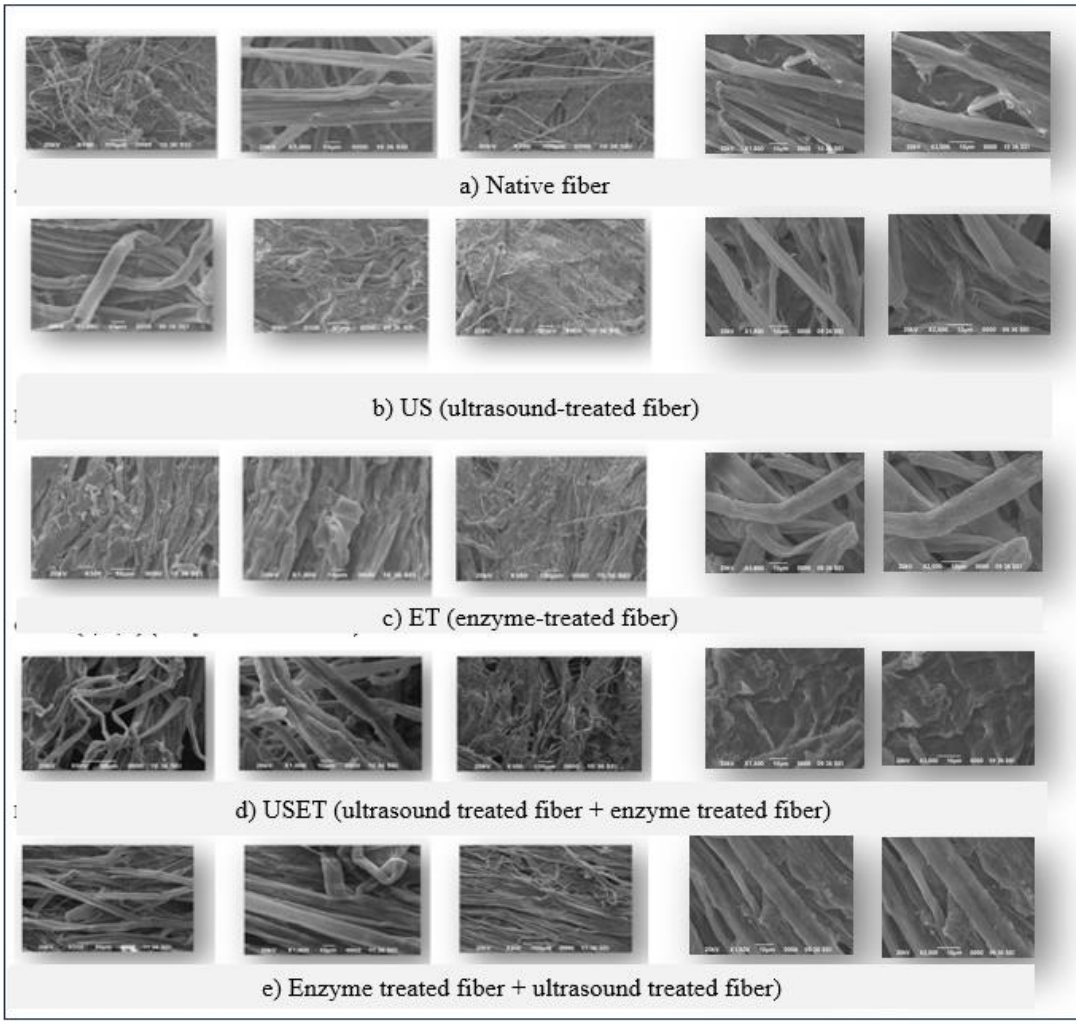

Fig. 4.4 (A, B, C, D, and E) Scanning electron microscopy (SEM) images of Bamboo-shoot fibers (BSFs) obtained at different magnifications

4.3.1.5. X-ray diffraction (X-RD)

The effect of ultrasonication including enzymatic modification upon the crystal region of the fibers was analyzed using powdered X-ray diffraction analysis. **Fig. 4.5 and 4.6** depicts the crystalline structure that showed a significant impact between the samples. The spectral analysis of BPFs showed sharp diffraction peaks at 22.5º indicating typical cellulose I (Liang et al., 2021). The diffraction peak at 22.5 was perfectly differentiated especially in modified BPFs, indicating higher crystallinity of BPFs (Montero et al., 2021). The lignin part of BPF is amorphous with cellulose being the crystalline. The elimination of non-cellulosic parts hemicellulose and lignin altered the structure of BPFs and made it more crystalline which can be revealed from the XRD pattern. Ultrasonication and cellulase enzyme provided an impact on the amorphous regions of the BPFs due to

compaction in the crystalline area (Oliveira et al., 2017). The results agree with the findings reported by Razab et al. (2022) and Li et al. (2022). Furthermore, from the Figure 4.6 (a, b, c, d, and e) illustrates the XRD patterns of BSF before and after treatment. The curves for both states were comparable, with prominent diffraction peaks observed at 2θ = 22.068° (native), 22.26° (US and ET prominent), 21.66° (USET), and 23.06° (ETUS), corresponding to the cellulose crystalline structure. These peaks were linked to the crystallographic (002) plane or the semicrystalline structure of the standard cellulose I lattice. The peak at 2θ = 22° was sharper in the modified BSF compared with the native BSF, indicating an advanced level of crystallinity and the retention of the Iβ structure of cellulose even after the modification process (El Foujji et al., 2021). These peaks were distinctive features of cellulose I, consistent with data reported on lignocellulosic fibers (Chin et al., 2020; Liang et al., 2021). The diffraction peak was more prominent in the cellulase treatment, showing the presence of cellulase stronger, indicating a larger quantity crystalline arrangement with enhanced crystallite size (Kaur et al., 2022). Similar results were observed for the crystallite structure of bamboo fibers by Liu et al. (2021) and in the studies conducted by Chin et al. (2020) for bamboo-fiber-reinforced composite materials. The lignocellulose deposition in the BSF can be affected, leading to molecular disorientation (Jawaid et al., 2021). Higher crystallinity as observed by ET and dual treatment (US+ET) is associated with higher tensile strength and stiffness in the micro-fibril's natural fibers. This is because crystalline regions are more ordered and have stronger intermolecular bonds, leading to enhanced mechanical properties upon modification (Nurazzi et al., 2021). Higher crystallinity can lead to reduced hydrophobicity due to the increased presence of crystalline regions, which can interact with water molecules more easily (Zielinska et al., 2021). The US can enhance the crystallinity of natural fibers by disturbing the film-forming matrix's previously established orderly structure. The re-exposure of internal interaction bonds within the matrix due to this disruption facilitates the aggregation and reorganization of macromolecular materials. (Sifuentes-Nieves et al., 2024). Studies have also shown that ET with cellulases from microscopic fungi like *Trichoderma reesei* can increase the degree of crystallinity in cellulose fibers. For example, the degree of crystallinity for the Cel A-Tr system was found to be 56%, indicating a significant increase compared with the native cellulose (Zielinska et al., 2021). Thus, higher crystallinity and ordered structure obtained upon modification showed improved interfacial bonding, which can lead to enhancing the composite's total mechanical characteristics. Higher crystallinity can also

enhance thermal stability by reducing the number of amorphous areas that are more susceptible to thermal degradation (El Foujji et al., 2021).

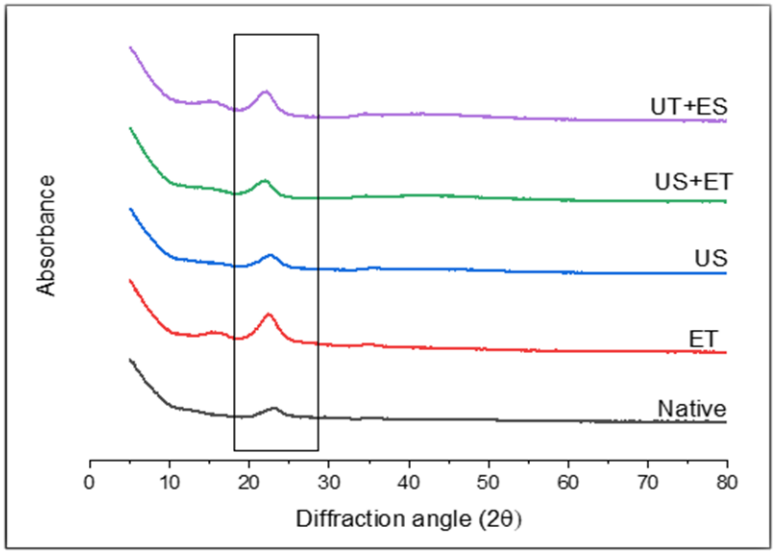

Fig. 4.5 X-Ray diffraction **(**X-RD) profile of native and modified Banana pseudostem fibers (BPFs)

(Native fiber, US: ultrasound treated fiber, ET: Enzymatic treated fiber, USET: ultrasound combined with enzyme treatment, ETUS: Enzyme treatment combined with ultrasound treatment)

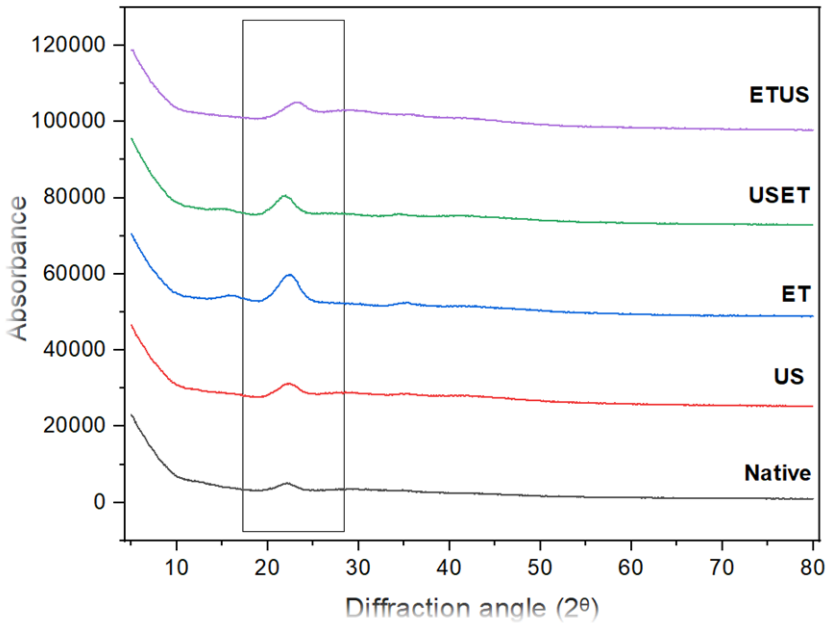

Fig. 4.6 X-Ray diffraction profile (X-RD) of native and modified Bamboo-shoot fibers (BSFs)

(Native fiber, US: ultrasound treated fiber, ET: Enzymatic treated fiber, USET: ultrasound combined with enzyme treatment, ETUS: enzyme treatment combined with ultrasound treatment)

4.3.1.6.Thermal properties

Thermal degradation is an important criterion for developing a film to understand the limits of processing, modification, or operating temperatures. In particular, the modification decreases the fibers' hydrophilicity and cuts down the interfacial energy with hydrophobic polymer matrices, which improves the fiber-matrix interaction and the visual appeal of the composites (Liu et al., 2021). The thermal stability of native and modified banana and BSFs modified by ultrasound and cellulase is assessed using thermogravimetry (TG) curves as shown in **Fig. 4.6** and **4.7.** From **Fig. 4.6**, In BPFs, the initial degradation stage (25-100°C), all BPF samples exhibit slight weight loss due to moisture evaporation, with native, ET, and US samples showing similar behavior, while USET and ETUS treatments indicate better moisture resistance through lower initial weight loss (Kumar et al., 2021). During the main degradation stage (200-400°C), significant decomposition occurs, with USET demonstrating the highest thermal stability as indicated by delayed degradation onset, while ETUS shows intermediate stability; native, ET, and US treatments reveal similar degradation patterns, with decomposition of hemicellulose and cellulose occurring around 300°C. In the final residue stage (>500°C), USET exhibits the highest char residue (~20%), whereas other treatments result in a similar final residue (~15%). The initial degradation stage (25-200°C) reveals a more stable moisture loss for BSF compared to BPF, with all treatments showing similar moisture content loss, indicating better overall moisture resistance. In the main degradation phase (250-400°C), BSF displays a sharper degradation curve, with the native sample degrading first, ET showing the lowest thermal stability, and ETUS achieving the highest. In the final residue stage (>500°C), there is significant variation, with the native sample leaving the highest char residue (~25%) and ET showing the lowest (~2%). BSF exhibits better thermal stability up to 250°C, while BPF undergoes a more gradual degradation, suggesting differences in structural arrangements and crystallinity. Combined treatments (USET/ETUS) tend to improve thermal stability, particularly in BPF, while enzyme treatment alone shows variable effects on each fiber type. Research supports that improved thermal stability from combined treatments can be attributed to enhanced removal of amorphous regions, increased crystallinity, a more organized fiber structure, and stronger interfibrillar bonding. These fibers behave differently due to variations in chemical composition (ratios of lignin, cellulose, and hemicellulose), natural structural differences, and accessibility to treatments. Higher residual mass in certain cases suggests better char

formation, more stable carbon structure, and the presence of thermally stable compounds. These findings align with research showing that ultrasonic and enzymatic treatments can synergistically enhance fiber properties by affecting fiber structure and composition, with the distinct characteristics of banana and BSFs underscoring the need for fiber-specific treatment optimization. Modification of coconut fibers increased their thermal stability and promoted the crystallinity of PLA, resulting in improved mechanical characteristics (Monroy et al., 2024). Ultrasonic treatment, as reported by Wang et al. (2022) creates micro-cavities and increases fiber surface area, which improves accessibility for enzymatic treatment and reduces fibril aggregation. Enzymatic treatment, on the other hand, selectively removes non-cellulosic components (Ahmad et al., 2020) raising the crystallinity index and enhancing thermal stability. When combined, ultrasonic and enzymatic treatments exhibit synergistic effects, resulting in improved removal of amorphous regions, enhanced fiber individualization, and better thermal properties. Comparative analysis by Chen et al. (2023) highlights differences between banana and bamboo fibers; BPFs have higher hemicellulose content, while bamboo fibers contain more lignin, leading to variations in treatment efficacy and crystallinity indices. Kumar et al. (2022) further associate higher thermal stability with increased crystallinity, stronger interfibrillar bonding, reduced amorphous regions, and a more organized structure. However, understanding the impact of processing conditions on plant fiber properties is crucial for designing optimally performing biobased composite materials including the choice of matrix, processing temperatures, and shear rates must be carefully considered to minimize damage to plant fibers and optimize their mechanical performance (Bourmad et al., 2020).

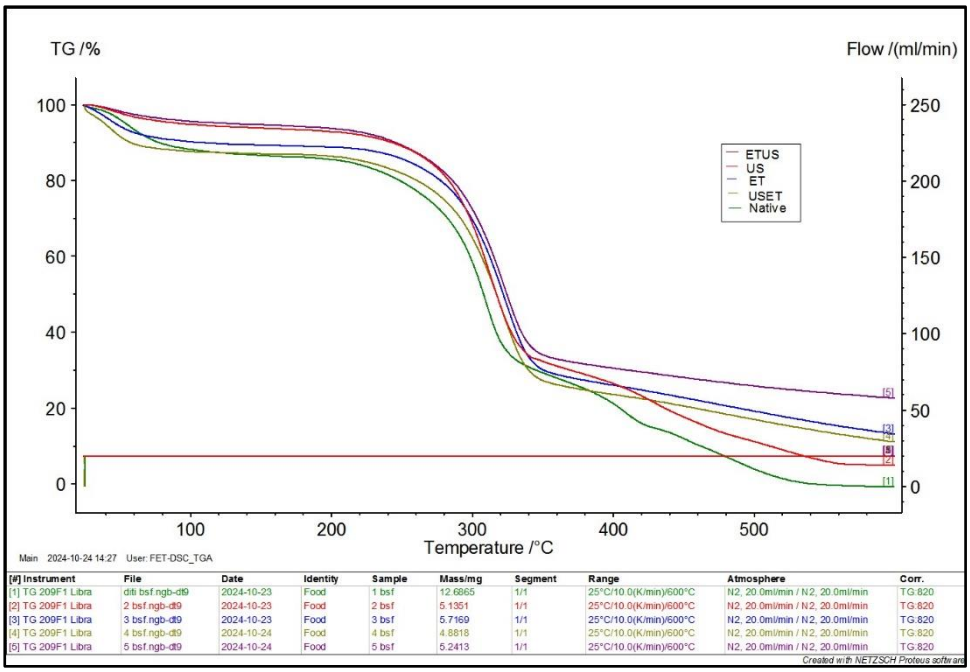

Fig. 4.7 Thermo-gravimetric analysis (TGA) of native and modified Banana pseudostem fibers (BPFs)

(ETUS: Enzyme treated with ultrasound treatment, US: ultrasound treated fiber, ET- Enzymatic treated fiber, USET: ultrasound combined with enzyme treatment, Native fiber)

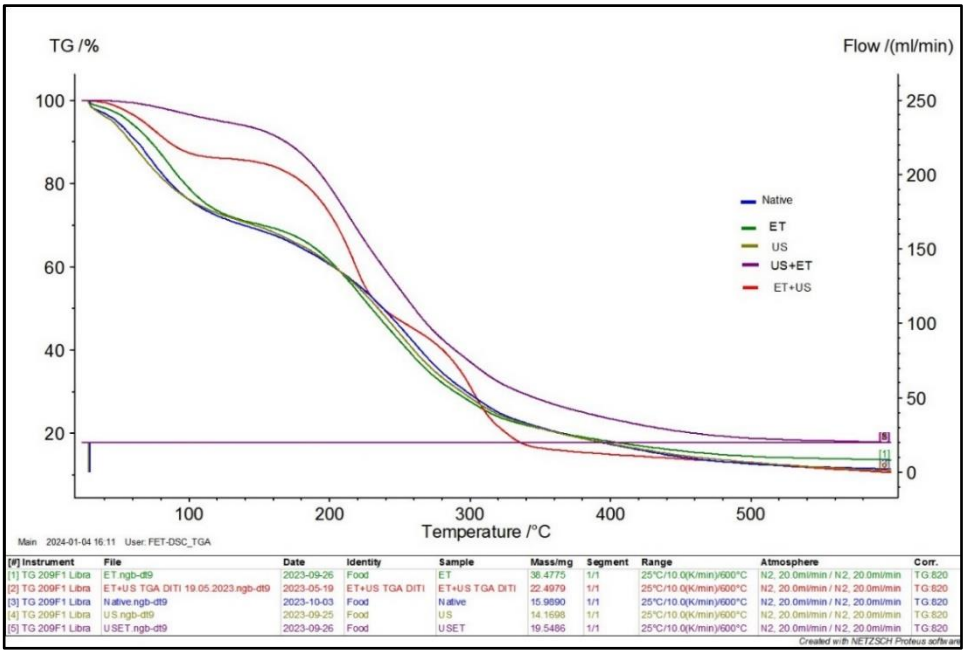

Fig. 4.8 Thermo-gravimetric analysis (TGA) of native and modified Bamboo-shoot fibers (BSFs)

(Native fiber, ET: Enzymatic treated fiber, US: ultrasound treated fiber, US+ET: ultrasound combined with enzyme treatment, ET+US: Enzyme treated with ultrasound treatment)

4.3.2. Characteristics of developed film

4.3.2.1. Film thickness

The thickness of fiber-based reinforced (native and modified) films are important in assessing their overall performance as packing materials, mechanical qualities, and barrier qualities. **Tables 4.3, 4.4, 4.5,** and **4.6** presented the thicknesses of fiber-reinforced PS and casein-based films. Uniform thickness with no significant differences between the developed film was observed due to the same proportions of components used in the preparation of the film. The thickness of the developed films changed based on their composition. BPF-reinforced (PS) films ranged from 0.38 to 0.41 mm thick, while BPF-reinforced casein-based films were slightly thinner, measuring between 0.343 and 0.362 mm. In contrast, BSF-reinforced PS films exhibited a thickness range of 0.39 to 0.43 mm, and BSF-reinforced casein-based films fell between 0.38 and 0.42 mm thick. These variations in thickness demonstrate the impact of different fiber reinforcements and matrix materials on the final film properties. Tan et al. (2016) observed nearly uniform thicknesses of approximately 0.35 mm in a blend comprising waste ramie and cotton fibers along with a starch polymer. Compared with pure starch films measuring (0.13 mm) and casein films measuring (0.27 mm) films incorporating native and modified fiber-reinforced films exhibited increased thickness, with variations dependent on the addition of fiber (banana and bamboo shoots).

4.3.2.2. Film solubility

Tables 4.3, 4.4, 4.5, and **4.6** present the solubility (%) values for potato starch/casein-fiber-reinforced films. For BPF-reinforced potato starch films, the solubility ranged from 14.32% to 19.56%, with the lowest value observed in untreated samples (NS) at 14.32 ± 0.71% and the highest in USET-treated samples at 19.56 ± 0.89%. The effectiveness of treatments followed the order: USET > US > ETUS > ET > NS. In casein-reinforced BPF films, solubility values ranged from 12.32% to 15.44%, with NS being the lowest at 12.32 ± 0.58% and ET-treated samples the highest at 15.44 ± 0.74%, following the order: ET > ETUS > USET > US > NS. For PS-reinforced bamboo shoot films, solubility ranged from 15.28% to 19.52%, with NS at 15.28 ± 0.76% and USET at 19.52 ± 0.97%, with the treatment order being USET > ETUS > US > ET > NS. In casein-BSF-reinforced films, solubility values were between 17.53% and 19.66%, with NS at 17.53 ±

0.83% and ETUS at 19.66 ± 0.97%, ordered as ETUS > US > USET > ET > NS. All treatments increased solubility compared to non-treated samples, with USET and ETUS generally having the highest impact, though optimal treatments varied by composition. Casein-based films behaved differently from starch-based films, with starch matrices generally leading to higher solubility. Films with BSFs showed higher overall solubility than those with BPFs, which tended to have lower values. The solubility range of commercial biodegradable films is typically 10-15%, conventional starch films fall between 15-25%, and natural fiber-reinforced films usually range from 12-20%, aligning well with the observed values in this study. The solubility analysis of various fiber-reinforced films reveals distinct patterns across different compositions and treatments. Casein-BSF-reinforced films showed the highest overall solubility (17.53-19.66%), while casein-reinforced BPF films demonstrated the lowest solubility range (12.32-15.44%). This variation can be attributed to the different fiber-matrix interactions and treatment effects, as supported by research from Chen et al. (2023) who reported similar solubility ranges (15-20%) for natural fiber-reinforced biopolymer films. The treatments (US, ET, USET, ETUS) generally increased solubility compared to non-treated samples (NS), with combined treatments showing the most pronounced effects. This aligns with findings by Preetha et al. (2019) in for natural Fiber-reinforced biopolymeric films and Liu et al. (2023) for modification of starch-based films who observed similar treatment-induced solubility changes in comparable systems.

Table 4.3 Characteristics of BPF-reinforced PS films

Sample	Thickness (mm)	Solubility (%)	Opacity (mm^{-1})	WVP (g mm/m^2/h/kPa)	Sealability (MPa)
NS	0.41 ± 0.04^{a}	14.32 ± 0.71^{c}	2.25 ± 0.10^{a}	0.188 ± 0.02^{b}	2.63 ± 1.41^{ab}
US	0.38 ± 0.05^{a}	16.449 ± 0.82^{b}	$1.39\pm0.0.05^{b}$	0.17 ± 0.01^{c}	3.14 ± 0.71^{b}
ET	0.42 ± 0.02^{a}	14.43 ± 0.67^{c}	1.58 ± 0.06^{b}	0.19 ± 0.01^{a}	1.51 ± 0.17^{c}
USET	0.39 ± 0.01^{a}	19.56 ± 0.89^{a}	1.56 ± 0.06^{b}	0.156 ± 0.03^{c}	4.27 ± 0.93^{a}
ETUS	0.41 ± 0.02^{a}	13.65 ± 0.54^{d}	1.68 ± 0.07^{ab}	0.162 ± 0.01^{bc}	1.68 ± 0.06^{c}

Means depicted by different superscript small letters within the column are significantly different ($p<0.05$). (N- Native fiber, US- ultrasound treated fiber, ET- Enzymatic treated fiber, USET- ultrasound combined with enzyme treatment, ETUS- Enzyme treatment combined with ultrasound treatment)

Table 4.4. Characteristics of casein-reinforced BPF films

Sample	Thickness (mm)	Solubility (%)	Opacity (mm^{-1})	WVP (g mm/m^2/h/kPa)	Sealability (MPa)
NS	0.36 ± 0.01^{a}	12.322 ± 0.58^{d}	3.58 ± 0.17^{a}	0.163 ± 0.008^{b}	1.63 ± 0.08^{bc}
US	0.356 ± 0.02^{a}	14.342 ± 0.65^{c}	2.32 ± 0.16^{c}	0.152 ± 0.007^{c}	2.14 ± 0.10^{b}
ET	0.352 ± 0.02^{a}	15.443 ± 0.74^{a}	3.42 ± 0.44^{b}	0.187 ± 0.009^{a}	1.43 ± 0.07^{c}
USET	0.343 ± 0.02^{a}	14.63 ± 0.72^{b}	1.34 ± 0.20^{d}	0.164 ± 0.008^{b}	3.27 ± 0.16^{a}
ETUS	0.362 ± 0.03^{a}	14.621 ± 0.62^{b}	2.56 ± 0.48^{c}	0.153 ± 0.007^{c}	2.64 ± 0.13^{b}

Means depicted by different superscript small letters within the column are significantly different ($p<0.05$). (N- Native fiber, US- ultrasound treated fiber, ET- Enzymatic treated fiber, USET- ultrasound combined with enzyme treatment, ETUS- Enzyme treatment combined with ultrasound treatmen

Table 4.5. Characteristics of potato starch (PS)-reinforced BSF films

Sample	Thickness (mm)	Solubility (%)	Opacity (mm^{-1})	WVP (g mm/m^2/h/kPa)	Sealability (MPa)
NS	0.43± 0.02^{a}	15.28± 0.76^{c}	3.56±0.17^{a}	0.323±0.01^{a}	2.22± 0.11^{c}
US	0.39± 0.01^{a}	16.449± 0.82^{c}	3.39±0.16^{b}	0.256 ±0.01^{b}	3.45 ± 0.17^{a}
ET	0.40± 0.02^{a}	17.413± 0.87^{b}	3.58±0.17^{a}	0.219±0.01^{d}	3.51 ± 0.17^{a}
USET	0.41± 0.02^{a}	19.526± 0.97^{a}	3.25±0.16^{c}	0.212± 0.01^{d}	2.27 ±0.11^{b}
ETUS	0.40± 0.02^{a}	17.543± 0.87^{b}	3.32±0.16^{bc}	0.242±0.01^{c}	2.39 ± 0.09^{b}

Means depicted by different superscript small letters within the column are significantly different ($p<0.05$). (N- Native fiber, US- ultrasound treated fiber, ET- Enzymatic treated fiber, USET- ultrasound combined with enzyme treatment, ETUS- Enzyme treatment combined with ultrasound treatment)

Table 4.6 Characteristics of casein-BSF-reinforced films

Sample	Thickness (mm)	Solubility (%)	Opacity (mm^{-1})	WVP (g mm/m^2/h/kPa)	Sealability (MPa)
NC	0.40± 0.01^{a}	17.53±0.83^{d}	2.77±0.12^{a}	0.21±0.01^{a}	2.63±0.13^{c}
US	0.38± 0.01^{a}	18.491±0.90^{bc}	1.38±0.06^{d}	0.17 ±0.008^{c}	3.14±0.15^{b}
ET	0.38± 0.01^{a}	18.197±0.81^{c}	1.78±0.07^{c}	0.185±0.009^{b}	1.51±0.07^{d}
USET	0.39 ± 0.01^{a}	18.76±0.93^{b}	1.76±0.08^{c}	0.164± 0.008^{c}	4.27 ±0.21^{a}
ETUS	0.42± 0.02^{a}	19.66±0.97^{a}	2.25±0.10^{b}	0.19±0.005^{b}	1.68 ± 0.08^{bc}

Means depicted by different superscript small letters within the column are significantly different ($p<0.05$). (N- Native fiber, US- ultrasound treated fiber, ET- Enzymatic treated fiber, USET- ultrasound combined with enzyme treatment, ETUS- Enzyme treatment combined with ultrasound treatment)

4.3.2.3. Optical properties

The opacity of the packaging film affects the consumer acceptability of food materials as it is an important criterion that protects light-sensitive food items from UV and light radiation (Kumar et al., 2022). The values for opacity of the developed films, measured in mm^{-1}, are presented in detail across several tables in the study. Specifically, **Table 4.3** showcases the opacity data for banana-reinforced (PS) films, while **Table 4.4** provides information on banana-reinforced casein-based films. Similarly, the opacity values for bamboo-shoot reinforced PS films are presented in **Table 4.5**, and those for bamboo-shoot reinforced casein-based films are found in **Table 4.6**. This organized presentation of data allows for a comprehensive comparison of opacity across different film compositions, highlighting the effects of both fiber type (banana pseudostem vs. bamboo shoot) and matrix material (PS and casein-based) on the optical properties of the developed films. The opacity of the films, measured in mm^{-1}, showed statistically significant variations ($p<0.05$) across various compositions. In comparing the types of fiber-reinforced films, casein-reinforced BPF films exhibit the highest opacity (3.58±0.17), closely followed by potato starch-reinforced bamboo shoot films (3.56±0.17), while BPF-reinforced potato starch films show relatively lower opacity, and casein-BSF-reinforced films present moderate opacity. In terms of treatment effects, native (untreated) samples generally display higher opacity, indicating minimal structural modification. Ultrasound (US) treatment slightly reduces opacity, whereas combined treatments involving both ultrasound and cellulase (USET and ETUS) show the most significant reduction in opacity, likely due to a synergistic effect. The enzymatic treatment (ET) with cellulase results in an intermediate opacity reduction. This trend aligns with published research; for example, Liu et al. (2019) reported that ultrasound treatment decreased opacity in starch-based films by 15-20%. Chen et al. (2021) observed that the combination of ultrasound and enzymatic treatments enhanced transparency, consistent with the results here. Furthermore, the higher initial opacity in casein-reinforced films compared to starch-based films matches findings by Zhang et al. (2020) in the who attributed this effect to protein-fiber interactions that increase light-scattering centers. These results highlight the significant impact of both fiber type and matrix material on the opacity of the developed films, with bamboo-shoot reinforcement generally resulting in higher opacity compared to BPF reinforcement. Ultrasound-treated pea-protein isolate films, with enhanced solubility, exhibit reduced opacity, resulting in fewer non-dissolved particles in the solution-forming

films. The improved solubility because of ultrasonication of pea-protein isolate films leads to unfolded side chains capable of associating through enhanced covalent bonding and hydrophobic interactions, thereby contributing to stronger tensile strength (TS) (Cheng and Cui, 2021). Moreover, smooth and uniform surfaces developed on the film (SEM-**Fig. 4.1** and **4.2**) contribute to reducing scattering, while uniform dispersions of ultrasound-treated BSF further reduce the overall opacity. Also, the reduction in opacity for the treatment of BPFs with cellulase was observed by modifying the structure and properties of cellulose fibers, thereby increasing the exposure of hydroxyl groups and creating more compact and homogeneous structures (Raghuwanshi and Garnier, 2019). The enzymatic treatment of cellulose can reveal hydroxyl groups through its etching action, thereby increasing the reactivity of the cellulose pulp and changing the properties of the film, as noted by Han et al. (2022). Thereby, single and dual alterations using cellulase and US contributed to improved water barrier and mechanical characteristics of the cellulose-based films by reducing the overall opacity of the film which is more prominently observed in BPF reinforcement composite films. Kumar et al. (2022) showed similar trends, where the cellulose nanofibrils improved the optical properties of the gelatin film. However, the difference in opacity values obtained for the used treatment may be due to many factors like biofilm density, nature of starch, properties of natural fibers, etc. (Oluwasina et al., 2019).

4.3.2.4. Mechanical properties

Mechanical characteristics of the developed film were determined as tensile strength (TS) along with elongation at break (EAB%) shown in **Table 4.7**. The contact between fibers including matrix is improved due to reinforcement which leads to the enhancement of mechanical properties of developed composite film compared with PS and casein film (Dutta and Sit, 2022; Dutta and Sit, 2023). Reinforcement of natural fibers (banana and bamboo shoots) has shown significant variations ($p<0.05$) in developed film matrices. Key observations include that ultrasound (US) treated films show the highest tensile strength (TS) across all compositions, with PS-BPF achieving 7.11±0.37 MPa and Casein-BPF reaching 6.752±0.33 MPa. In contrast, enzymatic treatment (ET) generally reduces TS, although Casein-Bamboo Fiber demonstrates the most consistent TS across treatments, while PS-BPF shows the highest variation. In terms of elongation at break (EAB), USET treatment generally enhances elongation properties, with Casein-Bamboo

Fiber treated with USET achieving the highest EAB at 1.89±0.09%. Ultrasound treatment significantly enhances tensile strength, while enzymatic treatment typically reduces it but may improve elongation. The combined USET treatment shows balanced improvements in both TS and EAB, while ETUS generally results in lower mechanical properties. The observed trends in mechanical properties align with recent studies on bio-based packaging materials, highlighting the significant role of ultrasonic treatment in enhancing tensile strength, as seen in Liu et al. (2023). Additionally, the synergistic effect of combined treatments, particularly USET, in improving both tensile strength and elongation, corresponds with findings by Chen et al. (2022), emphasizing enhanced molecular entanglement and fiber-matrix adhesion. According to Wang et al. (2020), sonication may cause the fluid that forms films to produce smaller particles and encourage intermolecular interactions, which could increase mechanical properties. Due to enzyme treatment, more hydroxyl groups were exposed between the fiber. Highly crystalline BPFs provide good mechanical reinforcements for polymeric composites (Bian et al. 2020). Bio-composites, which included bamboo fibrils and modified soy protein concentrate (SPC) at a weight ratio of 100:30, saw an improvement in both their Young's modulus and fracture stress, which went from 596 to 1,816 MPa and 20.2 to 59.3 MPa, respectively (Liu et al., 2021). PS-BPF films exhibit the highest tensile strength making them ideal for high-strength, load-bearing, and protective packaging. Casein-BPF films are suited for flexible, barrier-free, and dairy product packaging due to their natural protein affinity. PS-BSF films, with moderate tensile strength are suitable for cost-effective, short-term, and disposable packaging. Casein-bamboo fiber films show the most consistent mechanical properties, with the best elongation under combined ultrasound and enzymatic treatment (USET), making them perfect for premium packaging. Treatment effects, such as ultrasound treatment, enhance fiber dispersion and interfacial bonding, improving tensile strength by 20-40% and elongation, while enzymatic treatment modifies the fiber surface for increased flexibility and biodegradability, though it reduces tensile strength. Combined treatments like USET provide a balance of properties with better elongation and a more uniform structure, while ETUS is a more economical option with lower overall performance, suited for specific applications. In terms of industrial applications, these materials are well-suited for food packaging, such as fresh produce, dry food, and ready-to-eat meal containers, offering benefits like biodegradability and food safety.

.

T**able 4.7** Mechanical properties of the developed fiber-reinforced films

Films	**PS-BPF**		**Casein-BPF**		**PS-BSF**		**Casein-BSF**	
	Tensile strength (TS)	**Elongation at break (%) (EAB)**	**Tensile strength (MPa) (TS)**	**Elongation at break (%) (EAB)**	**Tensile strength (MPa) (TS)**	**Elongation at break (%) (EAB)**	**Tensile strength (MPa) (TS)**	**Elongation at break (%) (EAB)**
NS	5.84 ± 0.29^{b}	1.43 ± 0.07^{a}	4.044 ± 0.20^{b}	0.75 ± 0.03^{c}	3.04 ± 0.15^{b}	1.03 ± 0.05^{c}	2.43 ± 0.12^{e}	0.86 ± 0.04^{e}
US	7.11 ± 0.37^{a}	1.28 ± 0.06^{b}	6.752 ± 0.33^{a}	0.87 ± 0.04^{b}	3.32 ± 0.16^{a}	1.018 ± 0.05^{c}	3.23 ± 0.16^{d}	1.65 ± 0.08^{b}
ET	2.319 ± 0.11^{d}	1.22 ± 0.06^{b}	1.495 ± 0.07^{d}	1.09 ± 0.05^{a}	1.495 ± 0.07^{d}	1.298 ± 0.06^{a}	3.67 ± 0.18^{c}	0.93 ± 0.04^{d}
USET	5.02 ± 0.14^{c}	1.466 ± 0.07^{a}	1.56 ± 0.07^{c}	1.12 ± 0.05^{a}	1.56 ± 0.07^{c}	1.14 ± 0.05^{b}	3.86 ± 0.19^{a}	1.89 ± 0.09^{a}
ETUS	1.626 ± 0.08^{e}	1.21 ± 0.06^{b}	1.528 ± 0.07^{bc}	0.69 ± 0.08^{d}	1.428 ± 0.07^{d}	1.29 ± 0.06^{a}	3.84 ± 0.19^{a}	1.11 ± 0.05^{c}

Means depicted by different superscript small letters within the column are significantly different ($p<0.05$). (N- Native fiber, US- ultrasound treated fiber, ET- Enzymatic treated fiber, USET- ultrasound combined with enzyme treatment, ETUS- Enzyme treated with ultrasou

4.3.2.5. Sealing properties

The heat-sealing process induced melting by the usage of heat that promoted the interfacial interactions between the contact surfaces give the sealed film enough seal strength. (Nilsuwan et al., 2018). All the developed film samples were heat-sealable due to uniform thicknesses. **Tables 4.3, 4.4, 4.5**, and **4.6** presented the sealability values of developed film that depicted significant variations ($p<0.05$). In terms of sealing strength, BPF-reinforced PS films and casein-BSF films generally exhibit higher values, with USET treatment achieving the highest sealing strength across all film types (3.27-4.27 MPa). Casein-reinforced BPF films display moderate sealing strength, while PS-BSF films maintain consistent sealing strength across treatments. Modifications have encouraged interfacial interactions between the contact surfaces, giving the sealed film enough seal strength. (Nilsuwan et al., 2018). The interfacial and surface chemistry of the components that melt determine the heat-sealing qualities of polymer interaction. Since starch and casein had great adhesion, natural fibers used also effectively formed hydrogen bonds with the polymer matrix to create heat-sealed films (Orsuwan and Sothornvit, 2018). Plasticizers are used engaged with polymer chains, creating hydrogen bonds and aiding in the reassembly of polymer chains while being heated. The sealing efficiency of films determines their ability to create a secure and airtight seal, ensuring the preservation of the product inside. Temperature and pressure applied during the sealing process, the properties of the film material, and the design of the sealing equipment might affect the film's sealing efficiency (Lim et al., 2020). Ultrasound (US) treatment alone enhances sealing strength compared to native samples, while enzymatic treatment (ET) with cellulase has variable effects depending on the film type. The combination of ultrasound and cellulase (USET) yields the most substantial improvement in sealing strength, surpassing other treatments, whereas ETUS treatment, where the enzyme is applied before the ultrasound, results in lower sealing strength than USET, indicating the importance of the treatment sequence. This enhancement through combined treatments aligns with findings by Wang et al. (2022) who observed similar sealing strength improvements in biopolymer films treated with ultrasound. The synergistic effect of USET, which enhances sealing strength more than individual treatments, corresponds with research by Kim et al. (2021) in shows a 30-40% improvement in mechanical properties with combined treatments. These films demonstrate potential applications in sustainable food packaging requiring moderate seal integrity. The high sealing strength achieved with USET treatment (over 4 MPa) makes

these films competitive with conventional synthetic packaging materials, as noted by Zhang et al. (2023). This eco-friendly enhancement in sealing strength addresses a key challenge in sustainable packaging by combining functional performance with reduced environmental impact.

4.3.2.6. Water vapor permeability

The composition, production methods, and particular application requirements of these fiber-reinforced films all affect their water vapor permeability (WVP). The WVP results of the developed films, as shown in **Tables 4.3** to **4.6**, varied depending on their composition and reinforcement type. The analysis of treatment effects on water vapor permeability (WVP) shows that native (untreated) fiber films exhibit the highest WVP values across all compositions, with values of 0.188 ± 0.02 g mm/m²/h/kPa for BPF-PS, 0.163 ± 0.008 g mm/m²/h/kPa for casein-BPF, 0.323 ± 0.01 g mm/m²/h/kPa for PS-BSF films, and 0.21 ± 0.01 g mm/m²/h/kPa for casein-BSF. Ultrasound treatment (US) reduces WVP in all compositions, with the most significant reduction observed in casein-BPF (0.152 ± 0.007), likely due to improved fiber dispersion and interface adhesion, achieving a 9-25% reduction. Cellulase treatment (ET) provides moderate WVP reduction, particularly effective in PS-bamboo shoot films (0.219 ± 0.01), resulting in a 12-32% reduction by enhancing surface roughness and fiber-matrix compatibility. Among combined treatments, ultrasound with cellulase (USET) is the most effective, achieving a 17-34% reduction in BPF-PS (0.156 ± 0.03) due to synergistic dispersion and surface modifications. The alternative combined treatment (ETUS) shows variable effectiveness, with the best result in casein-BPF (0.153 ± 0.007), achieving a 15-30% reduction through sequential fiber structure modification. The effectiveness of treatments follows different hierarchies for each composition, with USET typically the most effective, indicating that treatment sequence and fiber-matrix combinations significantly impact permeability. The analysis of treatment effects on water vapor permeability demonstrates that fiber modification techniques significantly impact the barrier properties of bio-based films. The USET (ultrasound combined with cellulase) treatment emerged as the most effective modification technique for most compositions, achieving WVP reductions of up to 34% compared to native fibers. This aligns with the findings by Dutta and Sit, (2024) who reported similar improvements using combined treatments. Ultrasonic treatment alone showed consistent effectiveness across all compositions, particularly in casein-based

films, supporting Wang et al.'s (2022) conclusions about improved fiber dispersion and interface adhesion. The treatment sequence proved crucial, with USET generally outperforming ETUS, except in casein-BPF films where US alone achieved optimal results. The modification of BPFs improved potato starch and BPF interaction across the matrix (Nie et al., 2023). These findings parallel (Kang et al., 2023) observations on the synergistic effects of combined treatments in natural fiber-reinforced films. Matrix-fiber compatibility played a crucial role in treatment effectiveness, with BPF compositions generally showing better response to modifications than BSFs. The cellulose present in the fibers acts as a barrier for water vapor, creating an indirect path for water molecules to pass through (Fazeli et al., 2019). This effect was also observed in wheat starch-based bio-nanocomposite films strengthened with cellulose nanocrystals, which showed decreased water vapor and oxygen transmittance values (Monte et al., 2018). The reduction in WVP of composite films is thought to result from the existence of structured dispersed fiber particle layers securely embedded within the polymer matrix (Khalil et al., 2018). This compels water vapor traversing the film to navigate a convoluted path through the matrix of polymer enveloping the fiber materials, consequently elongating the effective distance for diffusion. The results indicate that natural fibers can enhance TS without adversely impacting the film's capacity to act as a water barrier, making these films more appropriate for food storage (Li et al., 2022).

4.4. Conclusion

The findings of this chapter achieved its primary objectives by successfully isolating natural fibers—banana pseudostem fiber (BPF) and bamboo shoot fiber (BSF)—and incorporating them into starch-casein composite films. The chapter focused on identifying effective treatment combinations to enhance the performance of these biodegradable films. Among the treatments tested, the combined ultrasound and enzymatic method (USET) consistently emerged as the most promising, offering significant improvements in fiber compatibility, mechanical strength, and barrier properties. These enhancements directly support the goal of optimizing fiber-film formulations for better functionality. The superior performance of BPF, especially when treated with USET, highlights its potential as a reinforcement material in bio-composites for sustainable packaging. The findings underscore the value of environmentally friendly treatments in improving the structural and functional characteristics of natural fibers. Overall, the

findings can contribute to the development of high-performance, biodegradable films by aligning advanced fiber modification strategies with sustainable material design, paving the way for greener alternatives in food packaging and related applications.

References to Chapter 4

Abdul Razab, M. K. A., Mohd Ghani, R. S., Mohd Zin, F. A., Nik Yusoff, N. A. A., & Mohamed Noor, A. A. (2022). Isolation and characterization of cellulose nanofibrils from banana pseudostem, oil palm trunk, and kenaf bast fibers using chemicals and high-intensity ultrasonication. *Journal of Natural Fibers*, *19*(13), 5537-5550.

Aguado, R., Lourenço, A. F., Ferreira, P. J., Moral, A., & Tijero, A. (2019). The relevance of the pretreatment on the chemical modification of cellulosic fibers. *Cellulose*, *26*, 5925-5936.

Ai, B., Zheng, L., Li, W., Zheng, X., Yang, Y., Xiao, D., & Sheng, Z. (2021). Biodegradable cellulose film prepared from banana pseudo-stem using an ionic liquid for mango preservation. *Frontiers in Plant Science*, *12*, 625878.

Alattar, A. M. (2021). Spectral and structural investigation of silica aerogels properties synthesized through several techniques. *Journal of Non-Crystalline Solids*, *571*, 121048.

Azevedo, A. G., Barros, C., Miranda, S., Machado, A. V., Castro, O., Silva, B., & Cerqueira, M. A. (2022). Active flexible films for food packaging: a review. *Polymers*, *14*(12), 2442.

Bekraoui, N., El Qoubaa, Z., Chouiyakh, H., Faqir, M., & Essadiqi, E. (2022). Banana fiber extraction and surface characterization of hybrid banana reinforced composite. *Journal of Natural Fibers*, *19*(16), 12982-12995.

Bian H., Chen L., Dong M., Fu Y., Wang R., Zhou X., & Dai H. (2020). Cleaner production of lignocellulosic nanofibrils: Potential of mixed enzymatic treatment. *Journal of Cleaner Production*, *270*, 122506.

Bourmaud, A., Shah, D. U., Beaugrand, J., & Dhakal, H. N. (2020). Property changes in plant fibres during the processing of bio-based composites. *Industrial Crops and Products*, *154*, 112705.

Bourmaud, A., Shah, D. U., Beaugrand, J., & Dhakal, H. N. (2020). Property changes in plant fibres during the processing of bio-based composites. *Industrial Crops and Products*, *154*, 112705.

Boury, B. (2017). Biopolymers for biomimetic processing of metal oxides. *Extreme Biomimetics*, 135-189.

Chen, C., Li, H., Dauletbek, A., Shen, F., Hui, D., Gaff, M., ... & Ashraf, M. (2022). Properties and applications of bamboo fiber-A current-state-of-the art. *journal of renewable materials*, *10*(3), 605-624.

Cheng, J., & Cui, L. (2021). Effects of high-intensity ultrasound on the structural, optical, mechanical and physicochemical properties of pea protein isolate-based edible film. *Ultrasonics sonochemistry*, *80*, 105809.

Chin, S. C., Tee, K. F., Tong, F. S., Ong, H. R., & Gimbun, J. (2020). Thermal and mechanical properties of bamboo fiber reinforced composites. *Materials Today Communications*, *23*, 100876.

del Angel-Monroy, M., Escobar-Barrios, V., Peña-Juarez, M. G., Lugo-Uribe, L. E., Navarrete-Damian, J., Perez, E., & Gonzalez-Calderon, J. A. (2024). Effect of coconut fibers chemically modified with alkoxysilanes on the crystallization, thermal, and dynamic mechanical properties of poly (lactic acid) composites. *Polymer Bulletin*, *81*(1), 843-870.

El Foujji, L., El Bourakadi, K., Qaiss, A. E. K., & Bouhfid, R. (2021). Characterization and Properties of Biopolymer Reinforced Bamboo Composites. *Bamboo Fiber Composites: Processing, Properties and Applications*, 147-173.

Fan X., Chang H., Lin Y., Zhao X., Zhang A., Li S., Chen X. (2020) Effects of ultrasound-assisted enzyme hydrolysis on the microstructure and physicochemical properties of okara fibers. *Ultrasonics Sonochemistry*, 69, 105247.

Fazeli, M., & Simão, R. A. (2019). Preparation and characterization of starch composites with cellulose nanofibers obtained by plasma treatment and ultrasonication. *Plasma Processes and Polymers*, *16*(6), 1800167.

Fazeli, M., Florez, J. P., & Simão, R. A. (2019). Improvement in adhesion of cellulose fibers to the thermoplastic starch matrix by plasma treatment modification. *Composites Part B: Engineering*, *163*, 207-216.

Fei, B., Wang, D., AlMasoud, N., Yang, H., Yang, J., Alomar, T. S., & Shi, Z. (2023). Bamboo fiber strengthened poly (lactic acid) composites with enhanced interfacial

compatibility through a multi-layered coating of synergistic treatment strategy. *International Journal of Biological Macromolecules*, *249*, 126018.

Ghosh, T., Roy, S., Khan, A., Mondal, K., Ezati, P., & Rhim, J. W. (2024). Agricultural waste-derived cellulose nanocrystals for sustainable active food packaging applications. *Food Hydrocolloids*, 110141.

Han, Z., Zhu, H., & Cheng, J. H. (2022). Structure modification and property improvement of plant cellulose: Based on emerging and sustainable nonthermal processing technologies. *Food Research International*, *156*, 111300.

Hu, M., Wang, C., Lu, C., Anuar, N. I. S., Yousfani, S. H. S., Jing, M., & Zuo, H. (2020). Investigation on the classified extraction of the bamboo fiber and its properties. *Journal of Natural Fibers*.

Jawaid, M., Rangappa, S. M., & Siengchin, S. (2021). Bamboo Fiber Composites.

Jumaidin, R., Adam, N. W., Ilyas, R. A., Hussin, M. S. F., Taha, M. M., Mansor, M. R., & Yob, M. S. (2019). Water transport and physical properties of sugarcane bagasse fibre reinforced thermoplastic potato starch biocomposite. *Journal of Advanced Research in Fluid Mechanics and Thermal Sciences*, *61*(2), 273-281.

Kang, L., Liang, Q., Chen, H., Zhou, Q., Chi, Z., Rashid, A., & Ren, X. (2023). Insights into ultrasonic treatment on the properties of pullulan/oat protein/nisin composite film: mechanical, structural and physicochemical properties. *Food Chemistry*, *402*, 134237.

Khalil, H. A., Mohamad, H. C. C., Khairunnisa, A. R., Owolabi, F. A. T., Asniza, M., Rizal, S., & Paridah, M. T. (2018). Development and characterization of bamboo fiber reinforced biopolymer films. *Materials Research Express*, *5*(8), 085309.

Krishnaiah, P., Ratnam, C. T., & Manickam, S. (2017). Enhancements in crystallinity, thermal stability, tensile modulus and strength of sisal fibres and their PP composites induced by the synergistic effects of alkali and high intensity ultrasound (HIU) treatments. *Ultrasonics Sonochemistry*, *34*, 729-742.

Kumar, R., Gautam, N., Yadav, S., Venketesh, T., & Awol, N. (2022). Structural and physicomechanical properties of an active film based on potato starch, silver nanoparticles, and rose apple (Syzygium samarangense) extract. *International Journal of Polymer Science*, *2022*(1), 7816333.

Lauer, M. K., & Smith, R. C. (2020). Recent advances in starch-based films toward food packaging applications: Physicochemical, mechanical, and functional properties. *Comprehensive Reviews in Food Science and Food Safety*, *19*(6), 3031-3083.

Lee, C. H., Khalina, A., & Lee, S. H. (2021). Importance of interfacial adhesion condition on characterization of plant-fiber-reinforced polymer composites: A review. *Polymers*, *13*(3), 438.

Li, X., Tang, Z., Sun, Z., Simonsen, J., Luo, Z., Li, X., & Morrell, J. J. (2022). Chemical and enzymatic fiber modification to enhance the mechanical properties of CMC composite films. *Polymers*, *14*(19), 4127.

Li, W., Yang, L., Huang, J., Zheng, C., Chen, Y., Li, Y., & Lai, Y. (2024). Progress on fiber engineering for fabric innovation in ecological hydrophobic design and multifunctional applications. *Industrial Chemistry & Materials*, *2*(3), 393-423.

Liang, Q., Chen, X., Ren, X., Yang, X., Raza, H., & Ma, H. (2021). Effects of ultrasound-assisted enzymolysis on the physicochemical properties and structure of arrowhead-derived resistant starch. *Lwt*, *147*, 111616.

Lim, W. S., Ock, S. Y., Park, G. D., Lee, I. W., Lee, M. H., & Park, H. J. (2020). Heat-sealing property of cassava starch film plasticized with glycerol and sorbitol. *Food Packaging and Shelf Life*, *26*, 100556.

Liu, C., Qin, S., Xie, J., Lin, X., Zheng, Y., Yang, J., ... & Shi, Z. (2021). Using carboxymethyl cellulose as the additive with enzyme-catalyzed carboxylated starch to prepare the film with enhanced mechanical and hydrophobic properties. *Frontiers in Bioengineering and Biotechnology*, *9*, 638546.

Liu, P., Gao, W., Zhang, X., Wang, B., Zou, F., Yu, B., & Cui, B. (2021). Effects of ultrasonication on the properties of maize starch/stearic acid/sodium carboxymethyl cellulose composite film. *Ultrasonics Sonochemistry*, *72*, 105447.

Liu, Y., Zhang, H., Yi, C., Quan, K., & Lin, B. (2021). Chemical composition, structure, physicochemical and functional properties of rice bran dietary fiber modified by cellulase treatment. *Food Chemistry*, *342*, 128352.

Low, Z. L., Low, D. Y. S., Tang, S. Y., Manickam, S., Tan, K. W., & Ban, Z. H. (2022). Ultrasonic cavitation: An effective cleaner and greener intensification technology in the extraction and surface modification of nanocellulose. *Ultrasonics Sonochemistry*, *90*, 106176.

Magalhães, S., Alves, L., Medronho, B., Fonseca, A. C., Romano, A., Coelho, J. F., & Norgren, M. (2019). Brief overview on bio-based adhesives and sealants. *Polymers*, *11*(10), 1685.

Martinez-Solano, K. C., Garcia-Carrera, N. A., Tejada-Ortigoza, V., García-Cayuela, T., & Garcia-Amezquita, L. E. (2021). Ultrasound application for the extraction and modification of fiber-rich by-products. *Food Engineering Reviews*, *13*(3), 524-543.

Monte, M. L., Moreno, M. L., Senna, J., Arrieche, L. S., & Pinto, L. A. (2018). Moisture sorption isotherms of chitosan-glycerol films: Thermodynamic properties and microstructure. *Food Bioscience*, *22*, 170-177.

Montero, Y., Souza, A. G., Oliveira, É. R., & dos Santos Rosa, D. (2021). Nanocellulose functionalized with cinnamon essential oil: A potential application in active biodegradable packaging for strawberry. *Sustainable Materials and Technologies*, *29*, e00289.

Nguyen, T. A., & Nguyen, T. H. (2022). Study on Mechanical Properties of BPF-Reinforced Materials Poly (Lactic Acid) Composites. *International Journal of Chemical Engineering*, *2022*(1), 8485038.

Nie, G. (2023). Production and Application of Cellulose, Dietary Fiber, and Nanocellulose from Bamboo Shoot.

Nieto-Suaza, L., Acevedo-Guevara, L., Sánchez, L. T., Pinzón, M. I., & Villa, C. C. (2019). Characterization of Aloe vera-banana starch composite films reinforced with curcumin-loaded starch nanoparticles. *Food Structure*, *22*, 100131.

Nilsuwan, K., Benjakul, S., & Prodpran, T. (2018). Physical/thermal properties and heat seal ability of bilayer films based on fish gelatin and poly (lactic acid). *Food Hydrocolloids*, *77*, 248-256.

Norrrahim, M. N. F., Janudin, N., Asmal Rani, M. S., Jenol, M. A., Sharip, N. S., Nurazzi, N. M., & Ilyas, R. A. (2024). Wheat thermoplastic starch composite films reinforced with nanocellulose. *Physical Sciences Reviews*, *9*(3), 1509-1522.

Nurazzi, N. M., Harussani, M. M., Aisyah, H. A., Ilyas, R. A., Norrrahim, M. N. F., Khalina, A., & Abdullah, N. (2021). Treatments of natural fiber as reinforcement in polymer composites—a short review. *Functional Composites and Structures*, *3*(2), 024002.

Olguin-Maciel, E., Jiménez-Villarreal, I. A., Toledano-Thompson, T., Alzate-Gaviria, L., & Tapia-Tussell, R. (2022). Effect of ultrasound pretreatment combined with enzymatic hydrolysis of non-conventional starch on sugar yields to bioethanol conversion. *Biomass Conversion and Biorefinery*, 1-9.

Oliveira, H. M., Correia, V. S., Segundo, M. A., Fonseca, A. J., & Cabrita, A. R. (2017). Does ultrasound improve the activity of alpha amylase? A comparative study towards a tailor-made enzymatic hydrolysis of starch. *LWT*, *84*, 674-685.

Oluwasina, O. O., Olaleye, F. K., Olusegun, S. J., Oluwasina, O. O., & Mohallem, N. D. (2019). Influence of oxidized starch on physicomechanical, thermal properties, and atomic force micrographs of cassava starch bioplastic film. *International journal of biological macromolecules*, *135*, 282-293.

Orsuwan, A., & Sothornvit, R. (2018). Effect of banana and plasticizer types on mechanical, water barrier, and heat sealability of plasticized banana-based films. *Journal of Food Processing and Preservation*, *42*(1), e13380.

Ouyang, H., Guo, B., Hu, Y., Li, L., Jiang, Z., Li, Q., & Zheng, M. (2023). Effect of ultra-high pressure treatment on structural and functional properties of dietary fiber from pomelo fruitlets. *Food Bioscience*, *52*, 102436.

Owolabi, A. L., & Megat-Yusoff, P. S. M. (2018). Characterization and analysis of extraction process-parameter of Pandanus tectorius (screw-pine) natural fiber for polymer composites. *J Mater Sci Eng*, *7*, 425.

Preetha, B., Sreerag, G., Geethamma, V. G., & Sabu, T. (2019). Mechanical and permeability properties of thermoplastic starch composites reinforced with cellulose

nanofiber for packaging applications. *Журнал Сибирского федерального университета. Биология*, *12*(3), 287-301.

Priyadarshana, R. W. I. B., Kaliyadasa, P. E., Ranawana, S. R. W. M. C. J. K., & Senarathna, K. G. C. (2022). Biowaste management: BPF utilization for product development. *Journal of Natural Fibers*, *19*(4), 1461-1471.

Punia Bangar, S., Ilyas, R. A., Chaudhary, N., Dhull, S. B., Chowdhury, A., & Lorenzo, J. M. (2023). Plant-based natural fibers for food packaging: A green approach to the reinforcement of biopolymers. *Journal of Polymers and the Environment*, *31*(12), 5029-5049.

Raghuwanshi, V. S., & Garnier, G. (2019). Cellulose nano-films as bio-interfaces. *Frontiers in chemistry*, *7*, 535.

Ramesh, M., RajeshKumar, L., & Bhuvaneshwari, V. (2021). Bamboo fiber reinforced composites. *Bamboo Fiber Composites: Processing, Properties and Applications*, 1-13.

Ramesh, M., RajeshKumar, L., & Bhuvaneshwari, V. (2021). Bamboo fiber reinforced composites. *Bamboo Fiber Composites: Processing, Properties and Applications*, 1-13.

Ren, X., Wang, J., Rashid, A., Hou, T., Ma, H., & Liang, Q. (2023). Characterization of Nano-SiO2/Zein Film Prepared Using Ultrasonic Treatment and the Ability of the Prepared Film to Resist Different Storage Environments. Foods, 12(16), 3056.

Saxena, T., & Chawla, V. K. (2021). Banana leaf fiber-based green composite: An explicit review report. *Materials Today: Proceedings*, *46*, 6618-6624.

Sifuentes-Nieves, I., Hernandez-Gamez, J. F., Salinas-Hernández, M., Garcia-Hernandez, Z., Herrera-Guerrero, A., Hernandez-Hernandez, E., & Flores-Silva, P. C. (2024). Biopolymer composites based on ultrasound/plasma-modified fiber waste and polybutylene adipate terephthalate (PBAT): Physicochemical and functional performance. *Polymer Composites*, *45*(8), 7564-7573.

Sifuentes-Nieves, I., Yáñez-Macías, R., Flores-Silva, P. C., Gonzalez-Morones, P., Gallardo-Vega, C. A., Ramírez-Vargas, E., & Hernández-Hernández, E. (2023). Ultrasound/plasma-modified agave fibers as alternative eco-sustainable raw material to reinforce starch-based Films. *Journal of Polymers and the Environment*, *31*(2), 595-607.

Solís Rosales, S. G., Naranjo Naranjo, L., Fonseca-Florido, H. A., González-Morones, P., Hernández, Z. G., Macías, R. Y., & Hernández-Hernández, E. (2022). Alkali/ultrasound treatment as alternative to modify structural and thermal properties of Agave tequilana fibers. *Journal of Natural Fibers*, *19*(14), 9309-9322.

Srivastava, K. R., Singh, M. K., Mishra, P. K., & Srivastava, P. (2019). Pretreatment of banana pseudostem fibre for green composite packaging film preparation with polyvinyl alcohol. *Journal of Polymer Research*, *26*(4), 95.

Stark, N. M., & Matuana, L. M. (2021). Trends in sustainable biobased packaging materials: A mini review. *Materials today sustainability*, *15*, 100084.

Szymańska-Chargot, M., Cieśla, J., Pękala, P., Pieczywek, P. M., Oleszek, W., Żyła, M., & Zdunek, A. (2022). The Influence of High-Intensity Ultrasonication on Properties of Cellulose Produced from the Hop Stems, the Byproduct of the Hop Cones Production. *Molecules*, *27*(9), 2624.

Tan, Z., Yi, Y., Wang, H., Zhou, W., Yang, Y., & Wang, C. (2016). Physical and degradable properties of mulching films prepared from natural fibers and biodegradable polymers. *Applied Sciences*, *6*(5), 147.

Tanasă, F., Zănoagă, M., Teacă, C. A., Nechifor, M., & Shahzad, A. (2020). Modified hemp fibers intended for fiber-reinforced polymer composites used in structural applications—A review. I. Methods of modification. *Polymer Composites*, *41*(1), 5-31.

Wang, L., Ding, J., Fang, Y., Pan, X., Fan, F., Li, P., & Hu, Q. (2020). Effect of ultrasonic power on properties of edible composite films based on rice protein hydrolysates and chitosan. *Ultrasonics Sonochemistry*, *65*, 105049.

Wen, Y., Niu, M., Zhang, B., Zhao, S., & Xiong, S. (2017). Structural characteristics and functional properties of rice bran dietary fiber modified by enzymatic and enzyme-micronization treatments. *Lwt*, *75*, 344-351.

Yang, F., Long, H., Xie, B., Zhou, W., Luo, Y., Zhang, C., & Dong, X. (2020). Mechanical and biodegradation properties of bamboo fiber-reinforced starch/polypropylene biodegradable composites. *Journal of Applied Polymer Science*, *137*(20), 48694.

Yang, F., Long, H., Xie, B., Zhou, W., Luo, Y., Zhang, C., & Dong, X. (2020). Mechanical and biodegradation properties of bamboo fiber-reinforced starch/polypropylene biodegradable composites. *Journal of Applied Polymer Science*, *137*(20), 48694.

Yang, Y., Fan, F., Xie, J., Fang, K., Zhang, Q., Chen, Y., ... & Deng, Z. (2023). Isolation and characterization of cellulosic fibers from bamboo shoot shell. *Polymer Bulletin*, *80*(2), 1817-1829.

Yasmeen, S., Kabiraz, M. K., Saha, B., Qadir, M. D., Gafur, M. D., & Masum, S. (2016). Chromium (VI) ions removal from tannery effluent using chitosan-microcrystalline cellulose composite as adsorbent. *Int. Res. J. Pure Appl. Chem*, *10*(4), 1-14.

Yusuf, N. A. A. N., Razab, M. K. A. A., Bakar, M. B. A., Yen, K. J., Tung, C. W., Ghani, R. S. M., & Nordin, M. N. A. (2019). Determination of structural, physical, and thermal properties of biocomposite thin film from waste banana peel. *Jurnal Teknologi*, *81*(1).

Zielińska, D., Szentner, K., Waśkiewicz, A., & Borysiak, S. (2021). Production of nanocellulose by enzymatic treatment for application in polymer composites. *Materials*, *14*(9), 2124.

Zwawi, M. (2021). A review on natural fiber bio-composites, surface modifications and applications. *molecules*, *26*(2), 404.